Grain-Boundary Surface States of (Ba, Pb)TiO$_3$ Positive Temperature Coefficient Ceramics Doped with Different Additives and Its Influence on Electrical Properties

Liang-Fu Chen and Tseung-Yuen Tseng, *Senior Member, IEEE*

Abstract— The electrical properties of positive temperature coefficient of resistance (PTCR) ceramics of composition (Ba, Pb, La)TiO$_3$ prepared from commercial BaTiO$_3$ powders doped with different additives were studied. It was proposed here that different additives might have generated the corresponding number of possible surface states, such as, the segregation behavior of Mn ions (3d transition metal ions), oxygen adsorption reaction resulting from BN addition, the action of Ca replacing the Ti sites (Ca''_{Ti}), and the natural intrinsic defects (V''_{Ba}, V''_{Pb}). In general, some experimental derivations were also offered that majority of the surface states, which possessed their individual surface energy level, possibly coexisted onto the grain surface. Utilizing the concept of the coexistence of different types of surface states in the energy band, a satisfactory point-to-point agreement was obtained between the measured result and calculated values for the resistivity curve. Our experimental results were analyzed based on the terms of the Heywang-Jonker model and have shown that the assumption of a Hewang barrier was a reasonable approach for our set of samples; however, the distribution and types of grain-boundary acceptor states classification were required.

Index Terms— PTCR, surface states, electrical properties, additives, Heywang barrier.

I. INTRODUCTION

THE ELECTRICAL resistivity of polycrystalline BaTiO$_3$, when properly doped with either a trivalent (e.g., Y, La, or Sb) or a pentavalent element (e.g., Nb or Ta) [1]–[2], increases by many orders of magnitude near the ferroelectric transition temperature T_c, a behavior commonly referred to as the positive temperature coefficient of resistance (PTCR) effect. The onset temperature of PTCR materials can be shifted lower or higher by substituting Sr^{2+} or Pb^{2+} for Ba^{2+}. Such a property makes it useful in a variety of applications such as transistors, current limiters, and self-regulating heating elements [2].

It has long been established that the barium titanate PTCR phenomenon is a grain-boundary resistive effect [3]–[5]. Besides, the research of previous workers shows that even at temperatures well below the Curie point the electrical

resistance is ascribed to the contribution of grain boundaries resulting from the residual barrier heights. Among the theories proposed to explain the electrical property of the grain boundary, Hewang's model of viewing the potential in the depletion region as a Schottkey barrier type is the most widely accepted [3]. Its mechanism involved is based on the presence of surface acceptor states at the grain boundary, which causes a potential barrier to be formed as a result of the upward bending of the conduction band in the depletion region. Later, the model was modified by Jonker to involve the ferroelectric property present below T_c, to partly compensate the charge trapped in the boundary region, i.e., the simultaneous low resistance and low permittivity before the anomalous jump are achieved by the reduced potential barrier as a result of the spontaneous polarization effects [4].

With respect to the origin of the surface acceptor states, a series of investigations and theories had been launched in the past. Hewang assumed earlier that the surface states originated from the presence of segregated p-type impurities in the grain boundary region [3]. Next, Jonker suggested that oxygen adsorption was physically causing the surface states [4]. Later, Daniel et al., proposed an alternative model based on Ba vacancies acting as acceptors [6]. Moreover, Ihrig postulated that some of 3d transition elements, in particular Mn which decreases the bulk charge carrier density and provide the deepest acceptor levels, are incorporated additionally as acceptors [7]. More recently, an argument was also proposed that the ability of oxygen absorption, enhanced by the appearance of 3d transition metal ions, was the main cause of affecting the surface-state densities [19]. All the possible acceptor types proposed by these authors may have coexisted at the grain boundary region if they are doped on purpose or occur naturally. Considering the variety of possible acceptors—3d transition metal ions (Mn, Fe, Cu) [7], different gaseous species absorbed on the grain surface (F, Cl, O) [8], even intrinsic cation vacancies (V''_{Ba}, V''_{Pb}) [6], [9], [10]—it should appear more reasonable to assume that the acceptor states are actually distributed over a certain energy range.

Both Heywang and Jonker assumed monoenergetic levels for the grain boundary acceptors. Ihrig and Puschert [12], by assuming a simple rectangular distribution in energy, improved the agreement in resistivity near the PTC maximum between

TABLE I
SINTERING CONDITIONS AND PHYSICAL PROPERTIES OF THE SAMPLES

Sample symbol	Composition	Sintering condition	Density (g/cm^3)	Grain size (μm)
N-1	$Ba_{0.897}Pb_{0.1}La_{0.003}TiO_3$	1280°C-30 min	6.283	6.3
NC	$Ba_{0.897}Pb_{0.1}La_{0.003}Ti_{0.995}Ca_{0.005}O_3$	1200°C-30 min	5.742	1.37
NM	N-1 + 0.06 mol% Mn	1260°C-30 min	5.992	4.54
NB	N-1 + 4 mol% BN	1200°C-6 min	4.929	5.18
NBM	N-1 + 4 mol% BN +0.06 mol% Mn	1200°C-6 min	5.031	4.786
NBMC	NC+ 4 mol% BN+0.06 mol% Mn	1200°C-6 min	5.198	4.34

theoretical calculations and empirical data. However, there exists a considerable difference no matter above or below the PTC maximum. Except examining the compensating effect of ionized oxygen vacancies for the effective surface-state density, the purpose of the present study is to classify the possible acceptor types existing simultaneously at the grain boundary with different additives. Based on the Hewang-Jonker model and our plausible assumption of classification, a more clear and excellent agreement for the resistivity curve is then given. We will discuss them in detail in Section IV.

II. THREE FUNDAMENTAL PTCR EQUATIONS

Theories based on the Hewang-Jonker model provide the following mathematical representation of describing the PTCR phenomenon.

According to the theory of diffusion-drift across the Heywang barrier, the observed resistivity ρ_{dc} is represented by

$$\rho_{dc}(T) = \rho_g[1 + (bkT/de\phi)\exp(e\phi/kT)] \quad (1)$$

where T is the absolute temperature in K, e the electronic charge, k the Boltzmann constant, d the grain size derived from the scanning electron micrograph, $b = N_e/2n$ the barrier width, and $\rho_g = 1/ne\mu$, given that μ is the electron mobility $(0.5 \text{ cm}^2\text{V}^{-1}\text{s}^{-1})$, is the grain resistivity extracted from the high-frequency intercept in the complex impedance diagram [11]. The height of the potential barrier is given by

$$\phi(T) = eN_e^2/8\varepsilon_o\varepsilon_r n \quad (2)$$

where ε_o is the permittivity of free space, ε_r the relative dielectric constant in the depletion layer, n the charge carrier density derived from ρ_g value, and N_e the temperature-dependent density of the occupied acceptor states given by the Fermi distribution

$$N_e(T) = N_s/\{1 + \exp[E_f + e\phi(T) - E_s]/kT\} \quad (3)$$

where N_s is the acceptor-state density, E_s the energy difference of the acceptor level from the band edge, $E_f = kT\ln(N_c/n)$ the Fermi level, and $N_c = 1.56 \times 10^{22}$ cm^{-3} the effective density of states in the conduction band (equal to Ti density) [12]. By solving (1), (2), and (3), named here as three fundamental PTCR equations, we have the semi-quantitative description of the PTC effect in all the temperature range [13]. Under the assumption of a constant value for N_e and $e\phi \gg kT$ within $T_c < T < T_{\max}$ and according to the Curie-Weiss law that $1/\varepsilon_r$ increases with temperature for ferroelectric materials above T_c, a dramatic rising of the resistivity arising from

the factor of $\exp(e\phi/kT)$ can be obtained in (1). Once the increasing barrier height with the temperature is large enough to prompt the surface energy level to coincide with the Fermi level, the effective surface-state densities begin to depopulate (3), and then, reduce the extent of the rising of barrier height (2). The maximum of the resistivity is thus reduced. It should be noted that the parameter ε_r in (2) has to be assigned before the calculations of $\rho_{dc} - T$ dependence on measured $\varepsilon_m - T$ are made. From dielectric theory, as derived by Wernicke [20], ε_m is substituted for ε_r by the following relationship:

$$\varepsilon_m = \varepsilon_r(d/2b). \quad (4)$$

With (4) and $b = N_e/2n$, the barrier height in (2) can be expressed in the form of

$$\phi(T) = edN_e/8\varepsilon_o\varepsilon_m. \quad (5)$$

Utilizing these formulas listed in (1), (3), and (5) as our framework, the electrical properties and semiconducting parameters of our list of samples will be discussed systematically.

III. EXPERIMENT

A. Sample Preparation

The "normal" composition of $Ba_{0.897}Pb_{0.1}La_{0.003}TiO_3$ were prepared by the conventional solid-state reaction technique. Commercially available powders of $BaTiO_3$, PbO, La_2O_3, TiO_2 were intimately mixed in a plastic jar and mechanically ball milled for 24 h in de-ionized water with plastic-coated iron ball media. The milled slurry was then dried by an IR lamp. After they were calcined at 950 °C for 90 min in an Al_2O_3 crucible in air, the semiconducting PTC powders were ball milled again with an appropriate amount of BN used as the sintering aids. For the purpose of comparing with the electrical properties under different additives "normal" samples doped with suitable amounts of $CaCO_3$ (0.5 mol%) and $Mn(NO_3)_2\cdot6H_2O$ (0.06 mol%) were also prepared as listed in Table I.

The green pellets with nominal dimensions of 1 cm in diameter by 0.2 cm thick were formed under 900 psi pressure. The respective compacts, covered by the same compositional powders, were then stacked inside a crucible with lids tightly fitted. The sintering condition, ranging from 1200 °C (6 min) to 1280 °C (30 min), were employed which were dependent on the sample's composition. The heating rate was fixed at 25 °C/min and the cooling rate was kept at 100 °C/h to 800 °C and then furnace cooling to room temperature. The scanning electron microscopy examination was carried out to observe
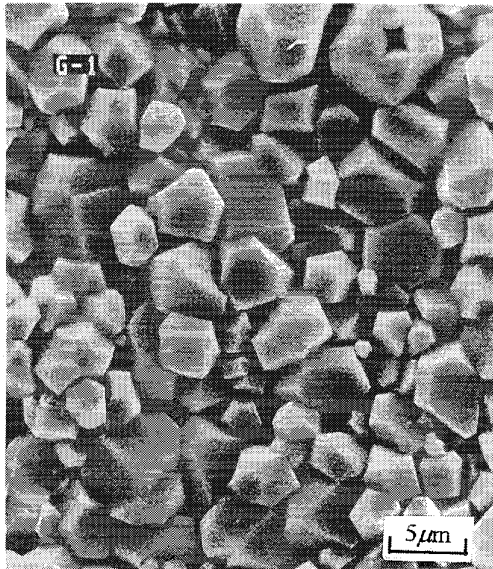
Fig. 1. Scanning electron micrograph of fracture surface of the sample NB.

Fig. 2. Relationship of the measured resistivity versus temperature for the samples with different additives.

the microstructure of the samples. Fig. 1 shows the scanning electron micrograph of fracture surfaces for merely BN-added sample. The average grain size was determined by the linear intercept method and the fired bulk density was obtained by Archimedes' techniques.

IV. ELECTRICAL MEASUREMENT

The electrical properties were measured by using a two-probe method from 40 °C to 550 °C in air by HP4140B (pA meter/dc voltage source) and HP4192A impedance analyzer at zero bias with AC signals amplitude of 1 V. Data was taken at frequencies ranging from 13 MHz down to 5 Hz, and corrected for lead inductance and stray residuals. Rubbed with In-Ga alloy (40:60) to ensure the ohmic contact at the ceramic-metal interface, the electrode surfaces of pellet were also covered with thin steel sheets pressed on to prevent the electrode material from vaporizing during heating. And then, samples were held in a programmable furnace heated at a rate of 3 °C/min and required enough time to equilibrate with surrounding temperature before each testing was made. It should be noted that the permittivity data was extracted at 100 kHz.

V. RESULTS AND DISCUSSION

Based on three fundamental equations, described in the previous section to extract various electrical parameters, a systematic comparison of electrical property and physical mechanism for our list of samples was completed:

The semiconducting PTC materials doped with different additives, usually a small amount, perform different R-T curves electrically. Fig. 2 indicates the relationship of resistivity versus temperature for these samples—N-1, NM, NC, and NB, respectively. Among these, the sample NB possesses the smallest density and the sample N-1 has the largest grain size as listed i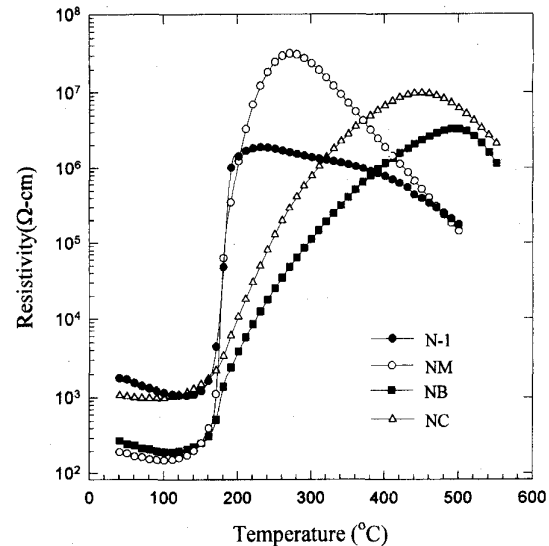n Table I. The incorporation of Mn is used as acceptor impurities to promote the PTC performance and the additions of Ca and BN are functioned as sintering aids to reduce the sintering temperature in the manufacturing process. It should be noted that the elements Mn and BN are doped additionally after forming the stoichiometry; however, the element Ca is substituted into the Ti sites to maintain the stoichiometry. Meanwhile, they possess individual sintering condition depending on the sample's composition as listed in Table I. We have observed four obviously different temperature coefficient of resistivity (TCR) between T_c and T_{max} (PTC maximum) on the basis of Fig. 2. The highest one is the sample N-1, and the smallest NB. Due to the apparent features concerning the different TCR and T_{max} values, it inspires our interest on that what roles they are playing for the PTC effect to show different R-T curves for different additives (Mn, Ca, BN). Basically, if the surface energy level is assumed single-level, we may conceive that as the surface-state level E_s approaches the Fermi level E_f with an increasing temperature near T_{max}, N_s starts to reduce progressively and resistivity reaches a maximum value. That is to say—if the position of the surface-state energy level from the conduction band locates deeper in the energy band, the temperature corresponding to the maximum resistivity would be extended further and results in more broad R-T curve. In order to determine the magnitude of N_s and E_s for demonstration, with ρ_{max}-T_{max} plots first shown by Jonker is made [8]. The ρ_{max} versus T_{max} plots are used to extract the surface parameters N_s and E_s based on the independent variables n and d. With the iterative method shown by Lai et al. [13] to determine ϕ and N_e from (3) and (5) and substituting them in (1), values of ρ_{max} and T_{max} are calculated for a range of E_s while N_s is kept constant. This is then repeated for other values of N_s until a map of (ρ_{max}, T_{max}) has been constructed for all E_s and N_s of interest. Fig. 3 illustrates the $\rho_{max} - T_{max}$ plots of the sample NM, from which one can obtain $E_s = 1.53$ eV and $N_s = 9.1 \times 10^{13}$ cm^{-2}. In a similar way, these values of the
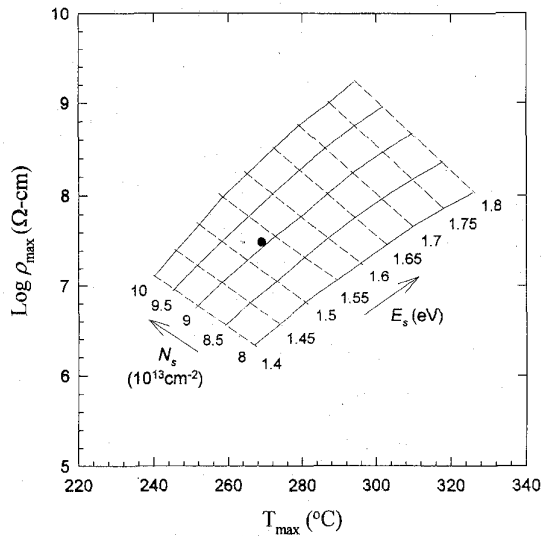
Fig. 3. Calculated $\rho_{\max}$ versus $T_{\max}$ plots for the sample NM. Solid dot represents the measured value.

Fig. 4. Measured resistivity-temperature characteristics of the samples, in which all the sintering conditions are kept the same.

TABLE II
RESISTIVITY MAXIMUM, TEMPERATURE AT THE PTC MAXIMUM, TEMPERATURE COEFFICIENT OF RESISTIVITY, ACCEPTOR STATE DENSITY, AND ENERGY DIFFERENCE OF THE ACCEPTOR LEVEL OF THE SAMPLES

Sample symbol	$\rho_{\max}$ ($\times 10^6$ Ω-cm)	$T_{\max}$(°C)	TCR (%/°C)	N_s ($\times 10^{13}$ cm^{-2})	E_s (eV)
N-1	1.8878	230	18.2	16.8	1.27
NM	31.483	270	13.9	7.18	1.53
NC	9.9316	450	5.76	2.84	1.76
NB	3.3159	490	4.13	1.42	1.89

other samples (N-1, NC, NB) can also be obtained and listed in Table II.

On the basis of Table II, we find that parameter N_s of these samples is not comparable because that the samples with various sintering conditions reflect naturally the different magnitudes of surface-state densities. The interesting parameter we focus on is the position of surface-state level (E_s) in the energy band. First, the composition of the sample N-1 which has no additions is (Ba, Pb, La)TiO$_3$ and its possible acceptor-like source should be merely cation vacancies (V''_{Ba}, V''_{Pb}) [6], [9–10]. Having just 10 mol% Pb content involved in it, most of the cation vacancies are dominated by V''_{Ba} and its corresponding surface energy level is 1.27 eV. Therefore, the lower $T_{\max}$ value is attributed to shallow energy level. Second, once the Mn impurities are added, raising the PTC jump order and inhibiting the grain growth, the resultant segregation behavior at the grain boundary makes the Mn ions to be the dominated surface states and shift the E_s value to 1.53 eV, i.e., a deeper level. Third, about the sample NC, calcium is used to substitute part of the Ti sites to form solid solution, which does not alter the cation stoichiometry, and Han et al. [15] have reported that calcium might be functioned as acceptor impurity. Therefore, we suppose that the dominated Ca$''_{Ti}$ acceptors are the major surface states causing low TCR value and its corresponding E_s value is 1.76 eV. Finally, the additive BN, either forming a liquid or volatilizing in air, is used as sintering aids to reduce the
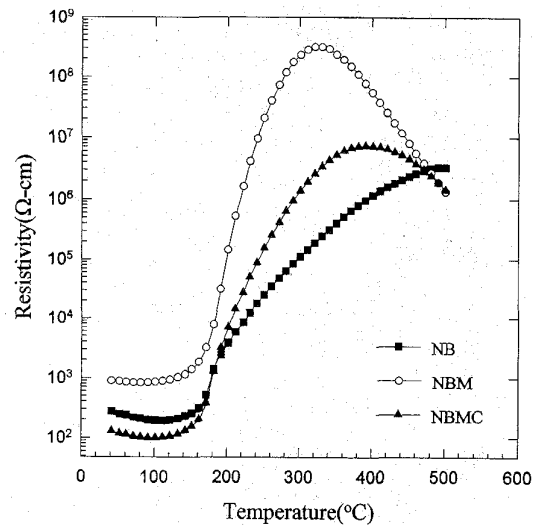
sintering temperature for the sample containing BN. Ho [16] has demonstrated that only a small amount of boron is retained at grain boundaries and claimed that the presence of B at a grain boundary is believed to promote the grain-boundary surface state (or acceptor-type state) density and thus enhances the PTC effect. On the other hand, the BN-added powders can be used to prepare the samples in a porous form (as shown in Table I, the samples containing BN have lower densities) to promote the penetration of oxygen, consequently enhance the oxygen adsorption and then increase the surface-state densities which enhance the PTC effect as suggested by Jonker [4]. Its corresponding E_s value is also shifted to 1.89 eV. In summary, we can conclude that a deeper energy level at the grain boundary leads to a higher $T_{\max}$ value. From our observation, the surface level of the BN-added sample is the deepest and its corresponding $T_{\max}$ value reaches highly 490 °C.

In order to ascertain the coexistence of the possible acceptor states described in Section I, we codope these additives randomly. The composition and physical properties of these samples (NB, NBM, NBMC) are listed in Table I. The sintering conditions of all the above samples are kept the same (1200 °C-6 min) to allow the electrical parameters (e.g., surface-state density, grain size, etc) to be comparable. Fig. 4 shows the resistivity-temperature characteristics of these samples, in which the NBM sample possesses the best PTC performance dominated by the amount of surface-state density at the grain boundary. To obtain the magnitude of N_s among them, an Arrhenius plot is made as the following. Approximating (1) by adopting (5) for the ϕ expression, the simplified (1) is expressed in the form of

$$\rho_{dc} = \rho_o \exp\left(e\phi/kT\right) = \rho_o \exp\left[AN_e/(\varepsilon_m T)\right] \qquad (6)$$

where ρ_o is assumed constant [17] and A is defined as

$$A = e^2 d/8\varepsilon_o k \qquad (7)$$

which is grain-size dependent constant. From (6), an Arrhenius plot of $\ln\left(\rho_{dc}\right)$ versus $\left(\varepsilon_m T\right)^{-1}$ is expected to exhibit a
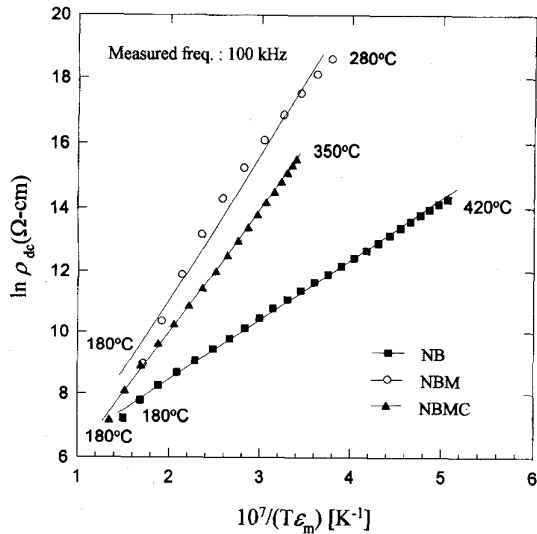
Fig. 5. Arrhenius plots of ln (ρ_{dc}) versus $(\varepsilon_m T)^{-1}$ for the samples.
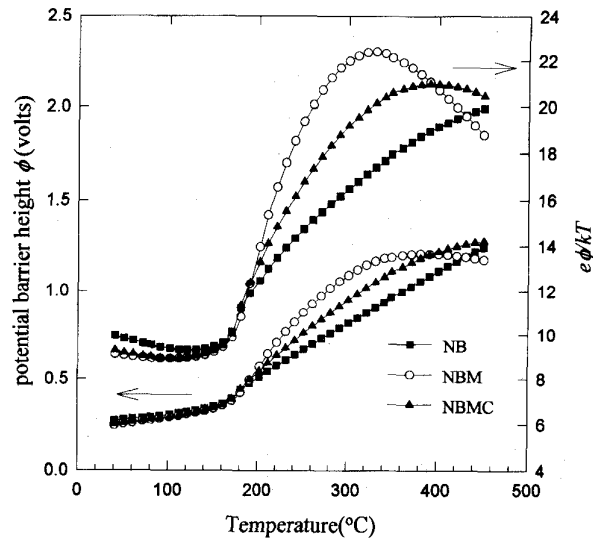

Fig. 6. Calculated barrier heights versus temperature curves for the samples. The grain-boundary phenomenon is implied by the $e\phi/kT$ versus temperature curve.

linear relationship with a constant N_e and the surface-state density N_s can be determined from the slope providing that the constant A is known. Fig. 5 shows the ln (ρ_{dc}) against $(\varepsilon_m T)^{-1}$ plots, in which all curves perform approximately the straight lines and the selected temperature region indicates the PTC range. However, the observed results are somewhat different from our expectation. The magnitude of surface-state density for these samples (NB, NBM, NBMC) are $1.42 \times 10^{13}, 3.62 \times 10^{13}$, and 3.48×10^{13} cm^{-2}, respectively, i.e., NBM > NBMC > NB. If the coexistence of different acceptor types at grain boundaries is mainly responsible for the observed results, the surface-state density of the sample NBMC, comprising Mn ions and Ca$''_{Ti}$ acceptors and interface states from oxygen adsorption, would be the largest, however, it is not. To explain this behavior, a defect chemistry is then proposed that oxygen vacancies would play an important role in causing such discrepancy. Al-Allak et al. [18] have assumed that ionized oxygen vacancies have an important effect of neutralizing some of the acceptor ions, thereby reducing their effective concentration. Comparing with these two samples NBM and NBMC, an inward mechanism is conducted that the negatively charged defect Ca$''_{Ti}$ is formed due to the incorporation of Ca on the Ti sites, and the corresponding number of positively charged oxygen vacancies will be required to satisfy the site balance and charge neutrality conditions [15].

$$\text{BaO} + \text{CaO} \rightarrow \text{Ba}_{\text{Ba}} + \text{Ca}''_{\text{Ti}} + 2\text{O}_o + \text{V}_o^{\cdot\cdot}. \qquad (8)$$
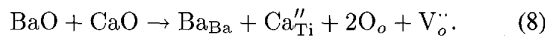
With increasing equilibrium concentration of ionized oxygen vacancies, more Mn ions or other acceptor ions are partly compensated, thus reducing the whole effective surface-state density.

When both the resistivity and permittivity data are known, the relation of barrier height versus temperature can be derived directly from solving (1) and (5) as shown in Fig. 6. Similarly, the sample NBM possesses the highest potential barrier height originating from larger N_s existing at the grain boundary for

all PTC range. It should be noted that the resistivity curve is controlled by the $e\phi/kT$ term, including the $T_{\max}$ and NTC characteristics below T_c and above $T_{\max}$. The calculated $e\phi/kT$ curve in Fig. 6 is analogous to the experimental ρ_{dc}-T relation which also implies that the PTCR effect is a grain-boundary phenomenon.

Therefore, as to the function of sintering aids, BN is better than Ca. Not only did the addition of BN reduce the sintering temperature to 1200 °C, but it also shortened the soaking time, and most importantly it doesn't eliminate the effective surface-state densities but, in fact, helps the reaction of oxygen adsorption to occur, and then promotes the PTC effect.

Finally, a calculated R-T curve will be examined to demonstrate the correctness of our concept of different additives resulting in different energy levels in the energy band. By applying the parameters derivation in Table II and the coexistence concept described above, the samples N-1, NM, and NBM are selected in understanding the physical mechanism. Based on three PTCR fundamental equations depicted in Section II and with the contribution of the $\rho_{\max}$-$T_{\max}$ plots, a calculated R-T curve can be obtained easily. At the beginning, the (E_s, N_s) pair is determined by the $\rho_{\max}$-$T_{\max}$ plots, and then, using the iterative method in solving (3) and (5) to obtain the relations of $\phi - T$ and $N_e - T$ if the $\varepsilon_m - T$ data is known, and finally, substituting these values into (1), the calculated resistivity data with temperature can be achieved [13]. Note that the resistivity curve below T_c can not be evaluated because of the complicated mechanism of the spontaneous polarization. Fig. 7 shows the calculated one of the sample N-1, in which an agreement in resistivity between T_c and $T_{\max}$ is satisfactory; however, a considerably large difference exists above PTC maximum. Note that (3) represents an assumption of single energy level which refers to cation vacancies (V$''_{\text{Ba}}$) for the sample N-1 here. Fig. 8 displays the calculated resistivity for the sample NM, in which the dashed line is under the
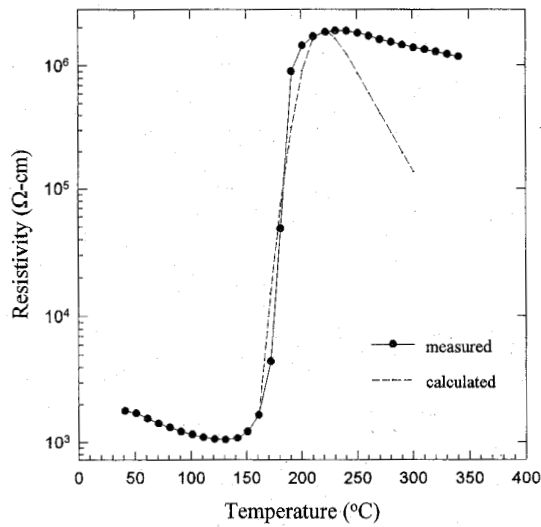
Fig. 7. Calculated and experimental resistivity versus temperature curves for the sample N-1.
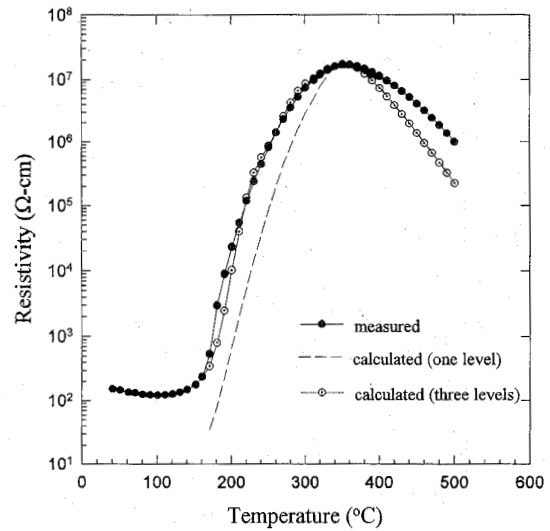

Fig. 9. Calculated and experimental resistivity versus temperature curves for the sample NBM. The empty symbol represents the postulation of three delta functions.
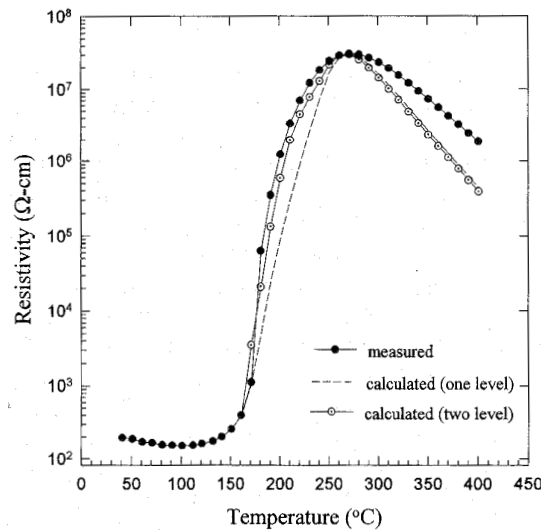

Fig. 8. Calculated and experimental resistivity versus temperature curves for the sample NM. The dashed line indicates the assumption of single energy level. Meanwhile, the empty symbol assumes two monoenergy levels involved in it.
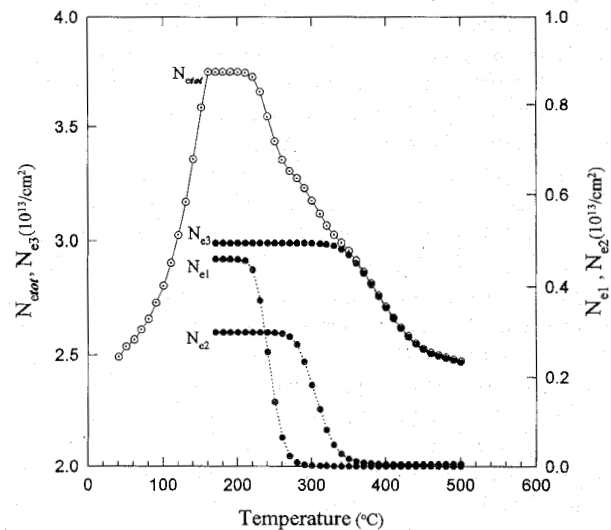

Fig. 10. Plots of the effective surface-state density against temperature. N_{e1}, N_{e2}, and N_{e3} indicate respectively the surface-state density of intrinsic cation vacancies, acceptor impurities, and interface states from the oxygen adsorption.

assumption of single level and has steeper slopes below and above the PTC maximum with the measured resistivity. To improve the agreement, the concept of energy coexistence described in Section I is utilized, that is to say, assuming two monoenergy levels existing simultaneously in the energy band. One belongs to cation vacancies (V''_{Ba}) and the other Mn ions. Apparently, this modification performs well within the $T_c \sim T_{max}$ region as shown in Fig. 8. Similar to that, three monoenergy levels, i.e., three delta distributions, are also assumed for the sample NBM and the result is shown in Fig. 9. The third additional energy level results from the oxygen adsorption due to the existence of boron at the grain boundary. Obviously, it performs as well as shown in Fig. 8. Once the distribution of surface energy levels are modified,

the effective surface-state density (N_e) is no longer expressed as the form of (3) but expressed as

$$N_e(T) = N_{e1} + N_{e2} + N_{e3}$$
$$= \frac{N_{S1}}{1 + \exp\left(\dfrac{E_f + e\phi - E_{S1}}{kT}\right)}$$
$$+ \frac{N_{S2}}{1 + \exp\left(\dfrac{E_f + e\phi - E_{S2}}{kT}\right)}$$
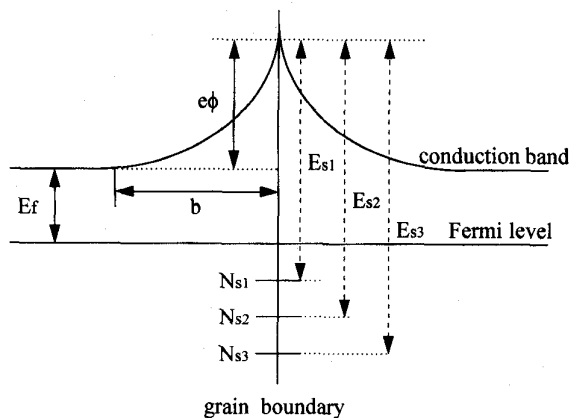$$+ \frac{N_{S3}}{1 + \exp\left(\dfrac{E_f + e\phi - E_{S3}}{kT}\right)} \qquad (9)$$

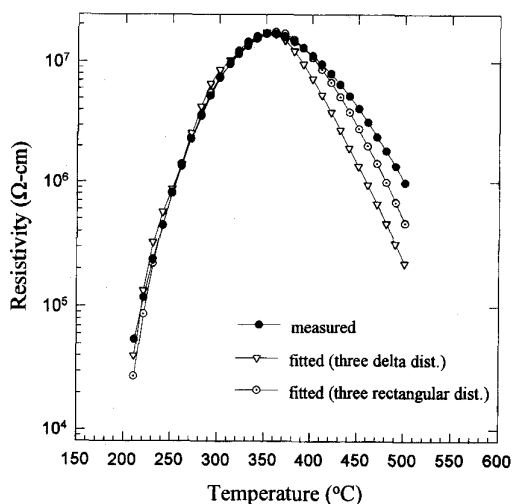Fig. 11. Modified energy band diagram of the Heywang barrier.

Fig. 12. Comparisons of the calculated and experimental resistivity curves under the assumptions of three delta distributions and three rectangular ones for the sample NBM.

where E_{s1}, E_{s2}, and E_{s3} represent, respectively, the surface energy level of intrinsic cation vacancies, acceptor impurities, and interface states from the oxygen adsorption. Notice that all the E_s values used above are the same as determined in Table II. N_{s1}, N_{s2}, and N_{s3} are then free parameters which must be adjusted to satisfy the best fitting with the measured resistivity. The distribution of these individual surface states with temperatures is shown in Fig. 10 and their representation of energy band diagram is also plotted in Fig. 11.

However, such modification of several monoenergy levels does not explain why the measured resistivity slope above the PTC maximum is less steep than the calculated slope. To solve it, the assertion of Ihrig and Puschert is adopted that surface states possess different energy levels distributed over a certain energy interval [12]. Therefore, we assumed a continuous distribution of the surface energy levels within a certain energy interval (Δ), i.e., three rectangular distributions. After assigning these free parameters (N_s, Δ) appropriately, an excellent agreement in resistivity below and above the PTC maximum is made as shown in Fig. 12.

VI. CONCLUSIONS

Based on the Heywang-Jonker model, we exploited three fundamental PTCR equations to handle related electrical parameters and made a systematical comparison and explanation for our system [(Ba, Pb, La)TiO₃+ additives]. Different additives generate different types of surface state at the grain boundary and have their own energy level depth. It is found that the deeper the surface energy level (E_s) is, the higher the T_{max} is on the basis of the ρ_{max}-T_{max} plots. The mere BN-added sample possesses the deepest surface energy level of 1.89 eV. And, with the use of Arrhenius plots of $\ln(\rho_{dc})$ versus $1/(\varepsilon_m T)$, we observed that ionized oxygen vacancies would neutralize the effective acceptor ions and then destroy the PTCR performance. Finally, a good agreement between the measured resistivity and calculated value is also made successfully by considering that different types of surface state which might be cation vacancies, acceptor impurities, or interface states from oxygen adsorption coexisted onto the grain boundary.

REFERENCES

[1] T. Murakami, T. Miyashita, M. Nakahara, and E. Sekine, "Effect of rare-earth ions on electrical conductivity of BaTiO₃ ceramics," *J. Am. Ceram. Soc.*, vol. 56, pp. 294–97, 1973.
[2] B. M. Kulwicki, "PTC materials technology, 1955–80," in *Advances in Ceramics, Grain Boundary Phenomena in Electronic Ceramics*, L. M. Levinson, Ed. Columbus, OH: American Ceramic Society, vol. 1, 1981, pp. 138–47.
[3] W. Heywang, "Barium titanate as a semiconductor with blocking layers," *Solid-State Electron.*, vol. 3, pp. 51–58, 1961.
[4] G. H. Jonker, "Some aspects of semiconducting barrium titanate," *Solid-State Electron.*, vol. 7, pp. 895–903, 1964.
[5] T. Y. Tseng and S. H. Wang, "ac electrical properties of high-curie-point barium-lead titanate PTCR ceramics," *Materials Lett.*, vol. 9, pp. 164, 1990.
[6] J. Daniels, K. H. Haerdtl, and R. Wernicke, "The PTC effect of barium titanate," *Philips Tech. Rev.*, vol. 38, pp. 73, 1978/1979.
[7] H. Ihrig, "PTC effect as a function of doping with 3d elements," *J. Am. Ceram. Soc.*, vol. 64, pp. 617–20, 1981.
[8] G. H. Jonker, "Halogen treatment of barium titanate semiconductors," *Mater. Res. Bull.*, vol. 2, pp. 401–07, 1967.
[9] G. Lewis and C. Catlow, "PTCR effect in BaTiO₃," *J. Am. Ceram. Soc.*, vol. 68, pp. 555–58, 1985.
[10] Y. Meng and X. L. Zhang, "Defect structure of (Ba, Pb)TiO₃ positive temperature coefficient ceramics and its influence on electrical properties," *IEEE Trans. Comp., Hybrids, Manufact. Technol.*, vol. 12, pp. 511, 1987.
[11] C. H. Lai and T. Y. Tseng, "Analysis of the AC electrical response for (Ba, Pb)TiO₃ positive temperature coefficient ceramics," *IEEE Trans. Comp., Packag., Manufact. Technol*, vol. 17, no. 2, pp. 309–315, 1994.
[12] H. Ihrig and W. Puschert, "A systematic experimental and theoretical investigation of the grain-boundary resistivities of *n*-doped BaTiO₃ ceramics," *J. Appl. Phys.*, vol. 48, pp. 3081–88, 1977.
[13] C. H. Lai, Y. Y. Lu and T. Y. Tseng, "Calculations and modeling of grain boundary acceptor states for (Ba, Pb)TiO₃ positive temperature coefficient ceramics," *J. Appl. Phys.*, vol. 74, p. 3383, 1993.
[14] J. Daniels and R. Wernicke, "New aspects of an improved PTC model," *Philips Res. Rep.*, vol. 31, pp. 544, 1976.
[15] Y. H. Han, J. B. Appleby, and D. M. Smyth, "Calcium as an acceptor impurity in BaTiO₃," *J. Am. Ceram. Soc.*, vol. 70, pp. 96–100, 1987.
[16] I. C. Ho, "Semiconducting barium titanate ceramics prepared by boron-containing liquid-phase sintering," *J. Am. Ceram. Soc.*, vol. 77, pp. 829–32, 1994.
[17] D. Y. Wang and K. Umeya, "Depletion-layer dielectric properties of positive temperature coefficient of resistance barium titanate," *J. Am. Ceram. Soc.*, vol. 73, pp. 1574–81, 1990.
[18] H. M. Al-Allak, A. W. Brinkman, G. J. Russell, and J. Woods, "The effect of Mn on the positive temperature coefficient of resistance characteristics of donor doped BaTiO₃ ceramics," *J. Appl. Phys.*, vol. 63, pp. 4530, 1988.

[19] A. B. Alles and V. L. Burdick, "Grain boundary oxidation in PTCR barium titanate thermistors," *J. Am. Ceram. Soc.*, vol. 76, pp. 401, 1993.
[20] R. Wernicke, "Two-layer model explaining the properties of SrTiO$_3$ boundary layer capacitors," in *Advances in Ceramics, Grain boundary Phenomena in Electronic Ceramics*, L. M. Levinson, Ed. Columbus, OH: American Ceramic Society, vol. 1, 1981, pp. 272–281.
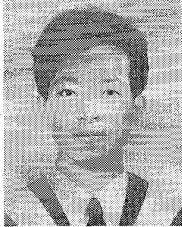
Liang-Fu Chen was born in Tainan, Taiwan, R.O.C., in 1971. He received the B.S. degree from the Department of Electronics Engineering, Chung-Yuan University, Chungli, Taiwan, R.O.C. and the M.S. degree from the Institute of Electronics, National Chiao-Tung University, Hsinchu, Taiwan, R.O.C., in 1993 and 1995, respectively.

During 1994–1995, he studied the physics of ferroelectric materials. His main research interest is in the area of electronic ceramics applications.
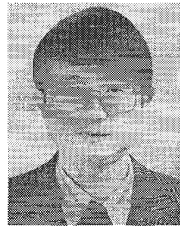
Tseung-Yuen Tseng (M'94–SM'94) received the Ph.D. degree in electro-ceramics from the School of Materials Engineering from Purdue University, West Lafayette, IN, in 1982.

Before joining National Chiao-Tung University, Hsinchu, Taiwan, R.O.C., in 1983, where he is now a Professor in the Department of Electronics Engineering and the Institute of Electronics, he was briefly associated with the University of Florida. His professional interests are electronic ceramics, ceramic sensors, and high-temperature ceramic superconductors. He has published more than 100 peer-reviewed technical papers, as well as presented 50 conference presentations.

Dr. Tseng was selected for inclusion in the Marquis *Who's Who in the World* in 1996 and is a member of the American Ceramic Society. In 1995, he received distinguished research award from the National Science Council of the Republic of China (R.O.C.).